^{13}N-Ammonia PET as a Measurement of Hindlimb Perfusion in a Mouse Model of Peripheral Artery Occlusive Disease

Iván Peñuelas[1,2], Xabier L. Aranguren[3,4], Gloria Abizanda[3,4], Josep María Martí-Climent[1], Maialen Uriz[3,4], Margarita Ecay[2], Maria Collantes[2], Gemma Quincoces[1], José A. Richter[1], and Felipe Prósper[3,4]

[1]Department of Nuclear Medicine, Clínica Universitaria, University of Navarra, Pamplona, Spain; [2]MicroPET Research Unit CIMA-CUN, University of Navarra, Pamplona, Spain; [3]Hematology and Cell Therapy Service, Clínica Universitaria, University of Navarra, Pamplona, Spain; and [4]Foundation for Applied Medical Research (FIMA), University of Navarra, Pamplona, Spain

Peripheral arterial occlusive disease (PAOD) is a leading cause of mortality and morbidity in the western world. The development of noninvasive methods for assessment and comparison of the efficacy of novel therapies in animal models is of great importance. **Methods:** Hindlimb ischemia was induced in nude mice by ligation and excision of the left femoral artery ($n = 5$) or the left iliac artery ($n = 10$). Assessment of limb perfusion was performed by small-animal PET analysis after intravenous injection of ^{13}N-ammonia between 24 h and 30 d after surgery using the ratio of perfusion between the left limb (ischemic) and the right limb (control). Activity concentration per area unit was calculated in regions of interest placed on 1-mm-thick images for numeric calculations, and the iliac and the femoral models were compared. In addition, histopathologic studies were performed to assess the degree of necrosis (hematoxylin−eosin) and fibrosis (sirius red). Immunohistochemistry analyses for identification of arterioles (α-smooth muscle actin) and endothelium—capillaries—(*Bandeiraea simplicifolia* I [BS-I] lectin) were also performed. **Results:** Perfusion in both hindlimbs of control animals was similar (median of the left-to-right ratio = 0.99). Twenty-four hours after ischemia, perfusion of the ischemic limb (% mean $\pm$ SD) was 33.3 $\pm$ 10.6 and 22.1 $\pm$ 9.9 in the femoral and iliac models, respectively. Spontaneous recovery of perfusion in the hindlimb that underwent surgery was significantly lower in the iliac model at day +15 (73.2 $\pm$ 15.5 vs. 51.9 $\pm$ 11.3; $P < 0.01$). Fibrosis increased progressively until day +30, whereas muscle necrosis was maximal at day +7 with a moderate reduction by day +30. In accordance with this positive effect, there was a statistically significant increase in the area covered with smooth muscle-coated vessels (arterioles) at day +30 in comparison with day 7 ($P < 0.05$). In addition, a correlation between ^{13}N-ammonia uptake and the amount of necrosis ($r = -0.73$; $P = 0.06$) and fibrosis ($r = -0.67$; $P = 0.05$) at day +30 was found. **Conclusion:** ^{13}N-Ammonia imaging allows semiquantitative evaluation of hindlimb perfusion in surgical mouse models of acute hindlimb ischemia. Although spontaneous perfusion recovery is observed in both models, the iliac model shows a substantially lower recovery and is hence better suited for assessment of new therapeutic strategies for acute hindlimb ischemic disease.

Peripheral arterial occlusive disease (PAOD) includes a spectrum of clinical syndromes affecting approximately 15% of adults over 55 y old (*1,2*), and it is a leading cause of morbidity and mortality in the western world. Although PAOD includes ischemic problems due to obstruction of the arterial blood supply to many different organs such as heart, brain, or kidney, it is the circulation of the lower extremities that is most frequently involved, leading to the development of the 2 major presentations of PAOD—intermittent claudication and critical limb ischemia (*2*).

Therapeutic options for patients with peripheral arterial disease usually target general atherosclerotic risk factors (antiplatelet antagonists, cholesterol-lowering therapy) (*3,4*); however, improvement of tissue perfusion is not really the usual target of such therapies. Surgical revascularization is beneficial, especially in patients with focal obstructions but, unfortunately, obstructions at multiple levels are common in PAOD (*5*). Induction of therapeutic neovascularization with exogenous growth factors, gene therapy, and, more recently, by (stem) cell therapy appears as an attractive approach for no-option patients (*6,7*), although the initial enthusiasm about the delivery of single genes/proteins has been tempered by a series of negative results from randomized clinical trials (*8*).

New and more efficacious therapies are needed, which has led to the development of several animal models of PAOD for experimental assessment of such novel therapeutic approaches (*9*). Proper judgment of recovery after these treatments is usually performed by combination of molecular biology, histology, and functional tests (*10–12*). Noninvasive imaging technologies already play an important role in our ability to assess the success of such

therapies, but certain limitations must be overcome for their use in small rodents (*13*). In the clinical setting, Doppler ultrasonography, contrast angiography, and venography are the standard imaging modalities used today, but various nuclear medicine techniques have also been used (*14–17*). Experimentally, hindlimb perfusion is frequently assessed by laser Doppler perfusion imaging (*18*), a technique that can be useful to detect superficial flow deficits but is unlikely to provide reliable information when considering subtle changes in blood flow. High-resolution magnetic resonance angiography and spectroscopy (*19*) as well as other nuclear medicine techniques are promising strategies for assessment of tissue perfusion (*20*).

The goal of our study was to develop a noninvasive methodology using high-resolution PET with ^{13}N-ammonia for evaluation of perfusion in surgical mouse models of acute and subacute hindlimb ischemia and quantitatively measured spontaneous recovery of perfusion in the animals that underwent surgery by repeatedly imaging the same individuals a long time after intravenous injection of ^{13}N-ammonia. The development of this technique should provide a useful tool for assessment of new therapeutic strategies for limb ischemia.

MATERIALS AND METHODS

Animal Models of Hindlimb Ischemia

Male nude mice (Harlan Ibérica, S.L.), weighing 25–30 g, were used. The selection of a model of immunosuppressed animals was undertaken with the aim of having a validated model amenable to being used in xenogeneic stem cell transplantation studies. All animal procedures were approved by the University of Navarra Institutional Committee on Care and Use of Laboratory Animals.

Mice were anesthetized with a mixture of ketamine (75 mg/kg) and xylazine (10 mg/kg) intraperitoneally and underwent surgery under sterile conditions. Two different models were used for hindlimb ischemia: (a) For the femoral group (F group, $n = 5$), a longitudinal incision was made in the skin overlying the middle portion of the left hindlimb. The femoral artery was ligated both at its proximal end and at the point distally where it bifurcates into the saphenous and popliteal arteries with 7/0 nylon ligature, and the artery and all side branches were dissected and excised. (b) For the iliac group (I group, $n = 10$), a laparotomy was performed and the iliac arteries were localized just at the bifurcation of the abdominal aorta. The left iliac artery was then ligated proximal to bifurcation and distally close to the inguinal ligament with 7/0 nylon ligatures and excised. All animals received an antiinflammatory agent (Ketoprofen, 5 mg/kg subcutaneously) daily for 3 d and an antibiotic (enrofloxacin, 25 mg/kg, in drinking water) for 5 d after surgery.

PET Protocols

Mice were anesthetized with 2% isoflurane in 100% O$_2$ gas for ^{13}N-ammonia injection (75 MBq) in a tail vein and were kept under such condition during the entire study. To obtain better images of both forelegs and facilitate drawing of regions of interest (ROIs) and quantitative analysis, animals were placed on the scanner cradle as shown on Figure 1. A Mosaic (Philips Electronics) small-animal dedicated imaging tomograph was used for all studies. The scanner has an axial field of view (FOV) of 11.9 cm

and a transaxial FOV of 12.8 cm. The resolution is 2.1-mm full width at half maximum.

Sinograms were reconstructed using the 3-dimensional RAMLA algorithm (row-action maximization-likelihood algorithm)—a true 3-dimensional reconstruction (*21*)—with 2 iterations and a relaxation parameter of 0.024, into a 128×128 matrix with a 1-mm voxel size. Scanner efficiency normalization, dead time, and decay corrections were applied during reconstruction.

For intersubject variability studies, a 30-min-duration dynamic PET study was performed on 5 control animals (nonsurgical animals) by means of a list-mode acquisition that was initiated simultaneously to tracer injection. After reconstruction, the following framing was applied for quantification and graphic display: 4×15 s, 2×30 s, 5×60 s, 4×120 s, 3×300 s. For test–retest studies, nonsurgical control animals were studied 3 times each on 3 consecutive days. For this purpose, 20-min PET studies were performed 10 min after ^{13}N-ammonia injection. For longitudinal studies of perfusion evolution in surgical animals and comparisons between groups, mice were randomly assigned to either the F or the I group and underwent surgery as described. For all animals, 20-min-duration small-animal PET studies were performed 10 min after ^{13}N-ammonia injection. In this case, PET scans were performed 1, 7, and 15 d (F group) and, additionally, 30 d (I group) after surgery.

Quantitative Image Analysis

For quantitative analysis and further comparisons among subjects, evaluation of perfusion was performed as previously described (*22*) with slight modifications. Briefly, ROIs were drawn on coronal 1-mm-thick small-animal PET images over the hindlimbs, and activity concentration per area unit was calculated as a measurement of perfusion. The ratio between the left and right hindlimbs (nonischemic limb) was used for comparisons. For dynamic studies, data were exported to the PMOD software package for quantification. All further static studies were analyzed using the software provided with the Mosaic scanner.

Tissue Processing and Histologic Analysis

At different time points after ligation, mice were anesthetized and perfused with phosphate-buffered saline for 5 min, which was followed by perfusion of 4% paraformaldehyde for 5 additional minutes. After dissection, the muscles were fixed for an additional 12 h and processed for paraffin embedding. For all staining and analysis, 3-μm sections were used. Hematoxylin–eosin ([H&E] analysis of necrosis and regeneration) staining and sirius red (analysis of fibrosis) staining were performed as described (*23*). For immunohistochemistry analysis, antibodies against α-smooth muscle actin (α-SMC; Dako) for identification of arterioles and the *Bandeiraea simplicifolia* I (BS-I) (Sigma) lectin that recognized mouse endothelium (capillaries) were used. Pictures for morphometric analysis were taken using a Retiga EXi camera (Q Imaging) connected to a Nikon E800 microscope or a Zeiss Axio Imager connected to a Axiocam MRc5 camera (Zeiss), and analysis was performed using Image J, KS300 (Leica), or Openlab 3.1 (Improvision) software.

Statistical Analysis

For statistical analysis, the SPSS version 13.0 statistical analysis package was used. A mixed factorial design with the group (F group vs. I group) as an intersubject factor and the time after surgery as an intrasubject factor was considered. A univariant general lineal mode analysis with group and time as fixed factors
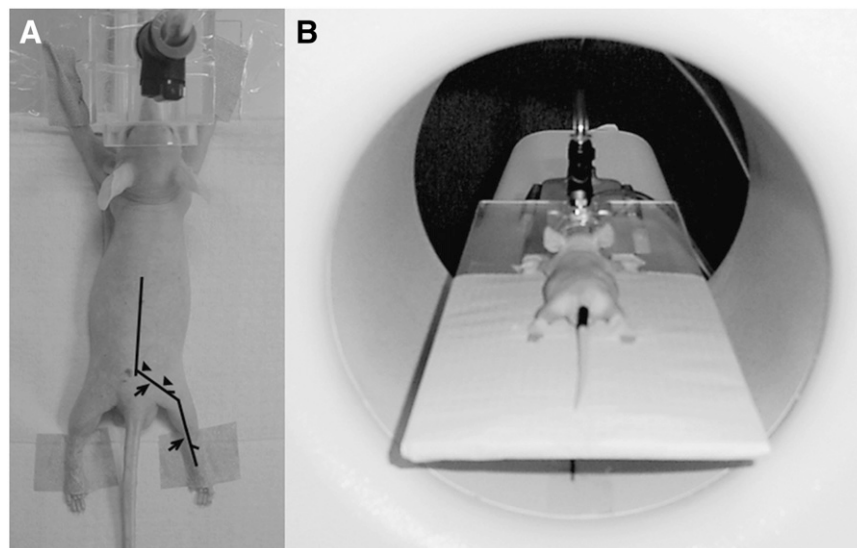
FIGURE 1. Animal placement in scanner for small-animal PET studies. (A) Lines represent iliac−femoral arteries showing where arteries were cut and excised (arrowheads, I model; arrows, F model). (B) Position of animal on cradle, illustrating position of legs of animals.

and animal as a random factor was used. The validity of the model was checked analyzing the normality of the residuals using the Shapiro–Wilk test. Tukey's HSD (Honestly Significant Differences) test was used for multiple a posteriori comparisons between time points. The Student t test for independent samples was used to analyze the differences between both groups in the 3 temporal measurements. For intragroup analysis of differences along time, the Wilcoxon test of the ranges was used. Correlations between small-animal PET and histopathologic data were analyzed using the Spearman correlation coefficients.

RESULTS

Hindlimb Perfusion in Control Animals and Repetition Studies

The plot in Figure 2 shows the mean $\pm$ SD of the ratio between both hindlimbs along the overall dynamic study (30 min). In low-flow areas (which is, in fact, the case for skeletal muscle), in which the tracer concentration in the vessels is high compared with that of the tissue, the integrals under the curves are, indeed, proportional to the
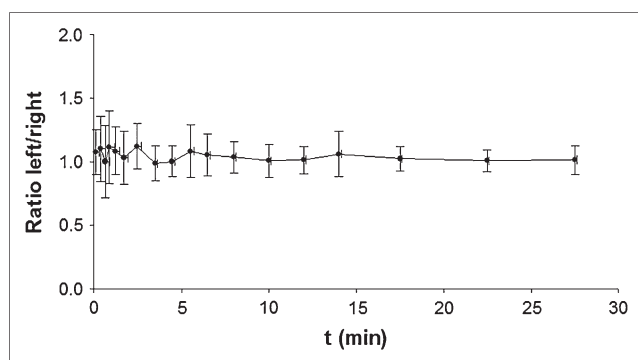

FIGURE 2. Left-to-right ratio of hindlimb perfusion (mean $\pm$ SD) in nonsurgical control animals ($n = 5$) as determined for dynamic PET studies. Data were acquired in list mode; framing was applied as described in the text and exported to PMOD software for numeric calculations. t = time.

absolute blood flow. Consequently, semiquantification in static images should therefore be possible using the healthy hindlimb as reference, obviating the need of an arterial input function. Hence, for further studies, we considered the time frame between 10 and 30 min to calculate quantitative values. In control animals, the median value of the ratio of ^{13}N-ammonia accumulation between left and right hindlimbs was 0.992 (range, 0.903–1.08). These results show that the perfusion of both legs is almost identical and, hence, it is possible to quantitatively evaluate perfusion by calculating the ratio between the surgical hindlimb and the contralateral limb in the time frame considered (10–30 min after injection).

Once we demonstrated that the perfusion of both legs was similar in nonsurgical control animals (and taking into account the planned follow-up studies), we then performed repeated studies. This was done to determine whether any variability due to the observer's ability to properly place the ROI for quantification in the appropriate plane could have any influence on the calculated numeric data. Numeric data were derived not only from a single plane but also from 3 ROIs drawn on 3 adjacent 1-mm-thick planes. Analysis of data demonstrated that there are no detectable differences among 3 studies performed on the same animals on different days. Furthermore, the results were similar considering either the mean value of the 3 planes analyzed (1.067; coefficient of variation [CV = 2.3%] or only one of them [1.057; CV = 2.9%]).

Perfusion Recovery in I and F Models

The fast recovery of perfusion in surgical mouse models of hindlimb ischemia is a well-documented fact that complicates the analysis of results derived from therapeutic angiogenesis procedures in such animals (24). Hence, a model with a slower spontaneous recovery of perfusion would definitively facilitate assessment of new therapies. Therefore, we compared 2 different surgical models of

hindlimb ischemia and measured perfusion for up to 1 mo after surgery by means of small-animal PET with ^{13}N-ammonia.

The Shapiro–Wilk test showed a normal distribution of the residuals, thus confirming that the statistical design used was appropriate. The univariant general lineal mode analysis with group and time as fixed factors and animal as a random factor showed no interaction between the fixed factors, thus showing that for both groups (I and F groups) there is a similar behavior along time. These results allow a global analysis of the main effects (group and time after surgery), showing that there are statistically significant differences ($P < 0.05$) between the F and I groups and that there are statistically significant differences ($P < 0.001$) among the different times. However, when we analyzed the differences between the I and F groups along time, no statistically significant differences could be found at days 1 and 7 between both groups, although there is a clear tendency of the I group to display lower perfusion recovery values compared with the F group (Fig. 3). However, at day 15, the perfusion in the I group is statistically lower ($P < 0.001$) than in that in the F group. The post hoc Tukey's test for multiple comparisons showed statistically significant differences ($P < 0.001$) between all paired time points analyzed (1 vs. 7 d, 1 vs. 15 d, and 7 vs. 15 d) (Figure 3). The signed Wilcoxon rank sum test for paired samples used for analysis of the differences along time within each group showed that there were statistically significant differences ($P < 0.05$) between any of the pairs of time analyzed for both the F and I groups (Table 1).
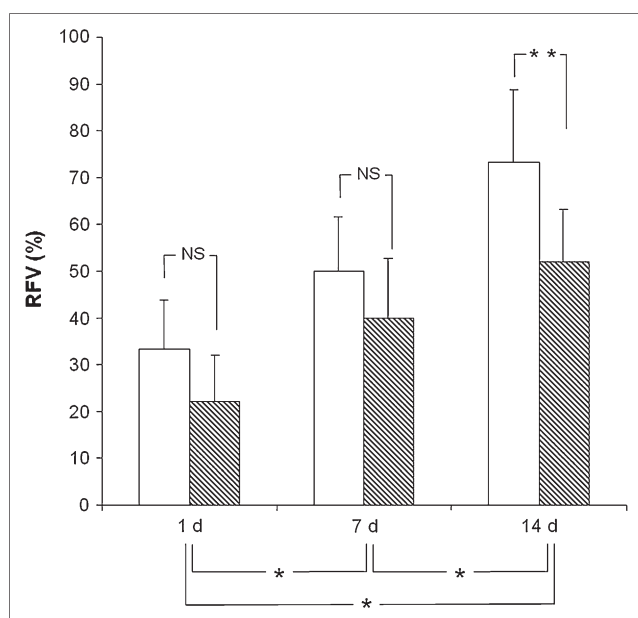

FIGURE 3. Comparison of spontaneous perfusion recovery along time between F model (white bars, $n = 5$) and I model (hatched bars, $n = 10$). NS = nonsignificant differences; RFV = relative flow values of ischemic vs. control hindlimb. *$P < 0.05$; **$P < 0.01$.

Images in Figure 4 clearly show that the surgical procedure results in a substantial decrease of perfusion in the surgical hindlimb. Spontaneous perfusion recovery was calculated as $100 \times (P2 - P1)/P1$, where P2 is the perfusion value on the second measurement date and P1 is the perfusion value on the first measurement date. Perfusion recovery was 80.2% in the first week after surgery, 30.1% between days +7 and +15, whereas it accounted for 27.1% between days 15 and 30 (Fig. 4), indicating that the recovery rate per day was almost 4 times faster in the first week than in the second week, showing an additional decrease in the following 15 d.

Histopathologic Studies

Expansion of the collateral bed in the adductor region is the most important backup mechanism to compensate for reduction in blood flow due to arterial obstruction in an effort to limit the necrosis and fibrosis of the muscle that is associated with reduced perfusion (25). As we have described, perfusion of the hindlimb recovers partially after hindlimb ischemia. To determine the effect of the ischemic lesion in the hindlimb and the spontaneous recovery, we quantified the amount of necrosis (H&E), of fibrosis (sirius red staining), and of vessels (capillaries and arterioles) at the different time points and compared these amounts with the right leg (nonischemic).

Whereas the amount of fibrosis increased progressively until day +30, muscle necrosis was maximum at day +7 and recovered slowly by day +30 (Figures 5 and 6). In accordance with this positive effect, there was a statistically significant increase in the area covered with smooth muscle–coated vessels (arterioles) at day +30 in comparison with day +7 ($P < 0.05$) (Fig. 6). Interestingly, the number of capillaries (per mm^2) was maximally reduced after 15 d following ischemia and then increased by day +30. A negative correlation between ^{13}N-ammonia uptake by small-animal PET and the amount of necrosis ($r = -0.73$; $P = 0.06$) and fibrosis ($r = -0.67$; $P = 0.05$) at day +30 was found. Although there was a correlation between ^{13}N-ammonia uptake and the α-actin area ($r = 0.488$) and the BS-I–positive structures ($r = -0.429$) at day +30, none of these correlations reached statistical significance.

DISCUSSION

PET with ^{13}N-ammonia to measure myocardial perfusion is a well-established technique that is routinely used in cardiac functional imaging (26). Procedures to determine the perfusion of highly perfused tissues (such as heart muscle) are usually performed on dynamic images obtained in the first minutes after the injection of ^{13}N-ammonia. On the other hand, in low-flow areas, a semiquantification in static images should be possible using the healthy hindlimb as reference.

However, ^{13}N-ammonia studies to measure perfusion on skeletal muscle have seldom been reported. In 1982, Schelstraete et al. (27) reported that, in a patient with a

TABLE 1
Statistical Comparison of ¹³N-Ammonia Uptake in Femoral and Iliac Hindlimb Ischemia Models

Group	Day +1 (% mean ± SD)*†	Day +7 (% mean ± SD)*†	Day +15 (% mean ± SD)*†	P
Femoral	33.29 ± 10.57 (21.88–47.82)	50.05 ± 11.58 (40.79–69.97)	73.23 ± 15.52 (47.49–86.75)	<0.01
Iliac	22.13 ± 9.93 (9.47–35.79)	39.87 ± 12.90 (16.45–61.46)	51.86 ± 11.35 (29.33–75.25)	<0.01

*Data are expressed as mean ± SD (range).
†Mean, SD, and ranges of percentage of perfusion of treated leg compared with contralateral leg.
P = comparison between ¹³N-ammonia uptake on day +1 vs. day +7, day +1 vs. day +15, and day +7 vs. day +15 for I group and F group.

right-sided static tremor, the high uptake of ¹³N-ammonia in the muscles of the right leg was related to increased perfusion produced by continuous exercise of the muscles involved in the tremor. More recently, Tack et al. (28) used ¹³N-ammonia PET to measure local perfusion in the legs of patients with painful diabetic neuropathy. Though ¹³N-ammonia PET measurements of perfusion in the extremities are not widely used, several nuclear medicine imaging procedures using other radiopharmaceuticals for perfusion measurements (²⁰¹Tl-chloride (15,29) or ⁹⁹mTc-methoxyisobutylisonitrile (14,17,22,30,31)) have been reported. These studies have demonstrated that nuclear imaging techniques are efficient methods to show lower-limb perfusion abnormalities.

The use of small-animal PET as a semiquantitative technique is easy to perform, does not require much computing expertise, and, hence, is available for any PET center. Furthermore, although small-animal SPECT devices today can reach equal or even better resolution than small-animal PET scanners, clinical PET provides a better resolution than SPECT, and the availability of a clinically useful method to quantify perfusion of the lower extremities in a relatively simple way would undoubtedly be very useful.

On the other hand, Doppler ultrasonography is the most widely used technique for these kind of studies but, as it has been stressed recently by Li et al. (32), laser Doppler is limited to measurement of superficial blood flow and,

hence, is inadequate to visualize, quantify, and characterize vascular development in response to the loss of a major arterial conduit, as is the case for usual animal models of hindlimb ischemia. Measurement of superficial blood flow is often considered as a measurement of perfusion in the analyzed structure, whereas both parameters cannot be considered equivalent in this kind of experimental study. In addition, Duet et al. (15) have shown that ²⁰¹Tl scintigraphy can detect lower-limb perfusion abnormalities in patients with normal Doppler pressure indices. Dabrowski et al. (30) have also shown that scintigraphic measurement of perfusion with ⁹⁹mTc-methoxyisobutylisonitrile yielded better agreement with the clinical evaluation than Doppler ultrasonography in patients with peripheral vascular disease of the lower extremities.

Considering all of these studies, we have reevaluated the available procedures to measure perfusion in the hindlimbs of small rodents and considered the ¹³N-ammonia imaging paradigm presented here as an adequate means of obtaining reliable measurements of perfusion in these experimental animal models. A main advantage of using ¹³N-ammonia is that we not only evaluate superficial blood flow, but rather perfusion of the whole muscle. The high correlation in the uptake between both hindlimbs, which allows us to establish the ratio between limbs as a perfusion measurement, and the extremely low variation in the repetition analysis, either considering a single ROI or 3 different ROIs, represent
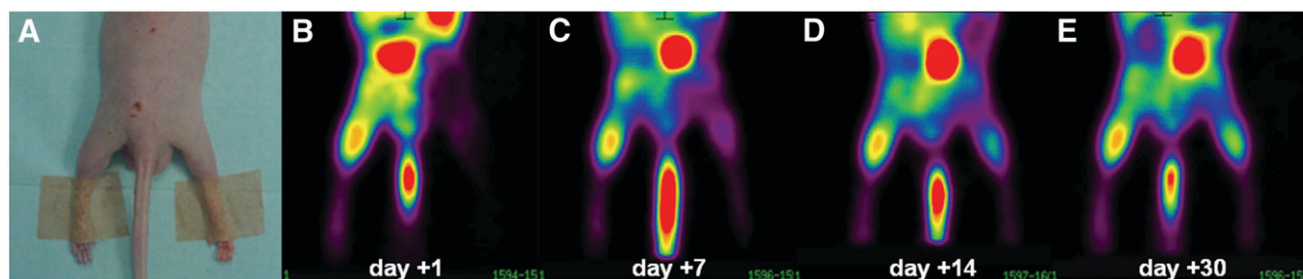

FIGURE 4. ¹³N-Ammonia small-animal PET images of spontaneous perfusion recovery in a representative animal after ligation of left iliac artery. Image in A shows a photograph of the hindlimbs of the animal to facilitate interpretation. Images in B–E correspond to the same animal studied 1, 7, 15, and 30 d after surgery. For this animal, perfusion of left hindlimb accounts for 10.3% (B), 28.6% (C), 51.0% (D), and 56.0% (E) of perfusion of nonsurgical contralateral hindlimb. Note spontaneous recovery of perfusion in left limb.
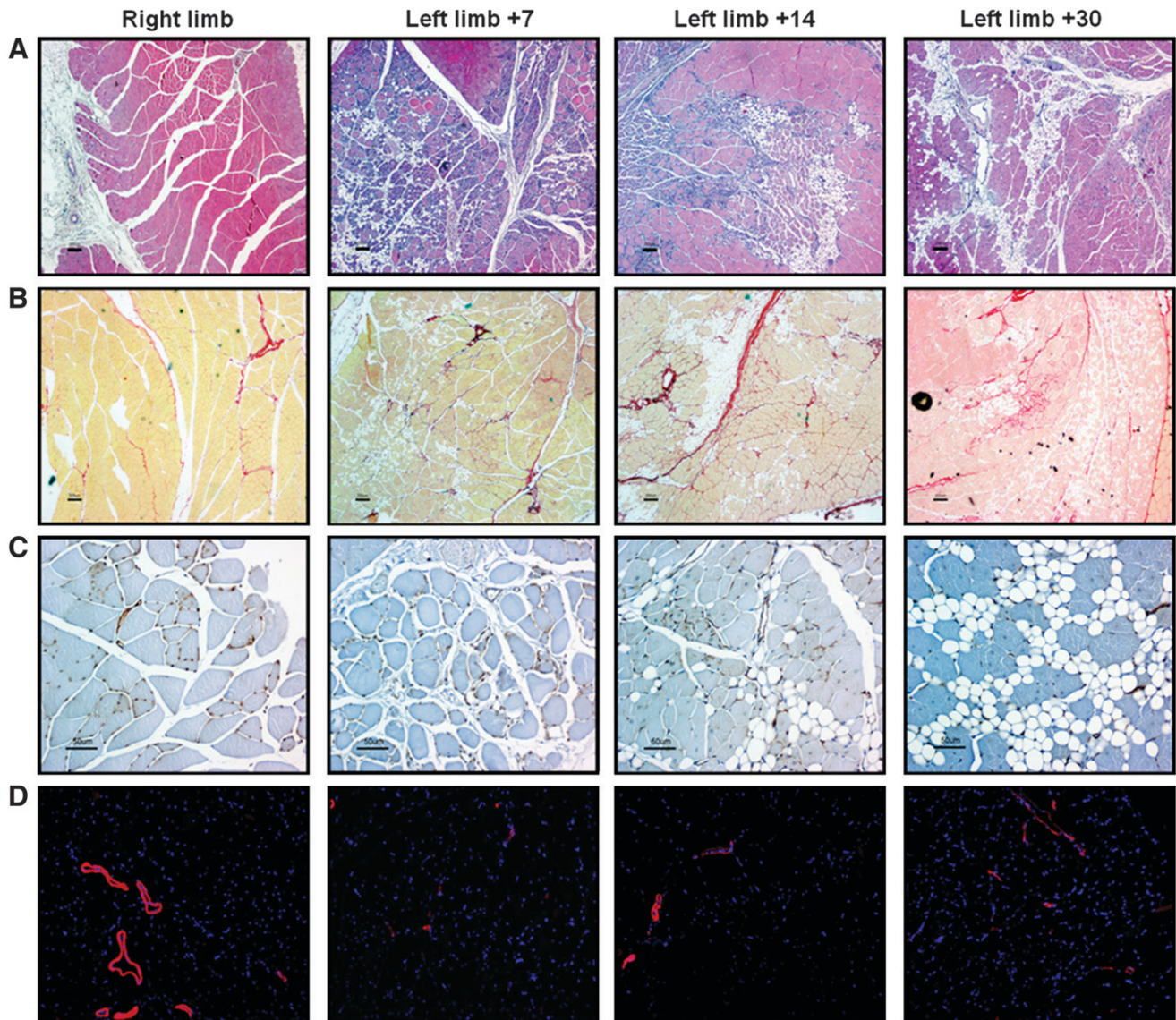
| | Right limb | Left limb +7 | Left limb +14 | Left limb +30 |

FIGURE 5. (A and B) Analysis of necrosis (defined by presence of fat cells and ''ghost'' muscle cells devoid of a nucleus) on H&E–stained cross-sections (A) and analysis of fibrosis on sirius red–stained cross-sections (B) of quadriceps muscles in right nonischemic limb and left ischemic limb at 7, 15, and 30 d after iliac artery ligation. (C and D) Analysis of vascular bed at capillary level (BS-I) (C) and arteriolar level (α-actin) (D) of quadriceps muscles in right nonischemic limb and left ischemic limb at 7, 15, and 30 d after iliac artery ligation. Scale bars: 200 μm (A and B), 50 μm (C), and $\times$200 (D).

a strength of this strategy for the quantitation of perfusion in models of hindlimb ischemia. The quality of the images obtained permits proper ROI delineation in both hindlimbs of the animals studied (Fig. 4). We show that, although there is almost an 80% reduction in perfusion in the ischemic leg 1 d after surgery, there is a fast recovery of perfusion during the first week that continues for at least 1 mo, albeit with a much slower progression rate (Figs. 4 and 5).

Another interesting finding of our study relates to the comparison of the 2 different models of limb ischemia. It is generally accepted that surgical models of limb ischemia show a spontaneous perfusion and functional recovery despite the persistence of some degree of muscular atrophy (*9,33*). When we analyzed both surgical models, we show

that, in both cases, perfusion is recovered progressively after surgery (Fig. 3; Table 1). Although the I model consistently shows lower perfusion recovery than the F model at days 1 and 7, from the statistical point of view no differences can be found between both groups. Further increases in the number of animals used might reduce the variability and lead to statistically significant differences between the groups. In any case, when perfusion is evaluated 2 wk after surgery, we can clearly observe that the I model is substantially better than the F model. An important caveat of most models of acute hindlimb ischemia is that human disease is usually a bilateral disease that is much more complex than the animal disease, where vascular obstructions develops gradually with involvement of multiple

FIGURE 6. (A and B) Quantification of necrotic (A) and fibrotic (B) area expressed as percentage vs. total muscle area of quadriceps muscle. (C and D) Quantification of microvascular vessels stained with BS-I (C) expressed as number of vessels by mm² of quadriceps muscle and arteriolar vessels (D) expressed as area positive for α-actin staining vs. total muscle area of quadriceps muscle. For histologic analysis, only animals in which left iliac artery was excised were used. Results represent mean ± SD. *$P < 0.05$; **$P < 0.01$.
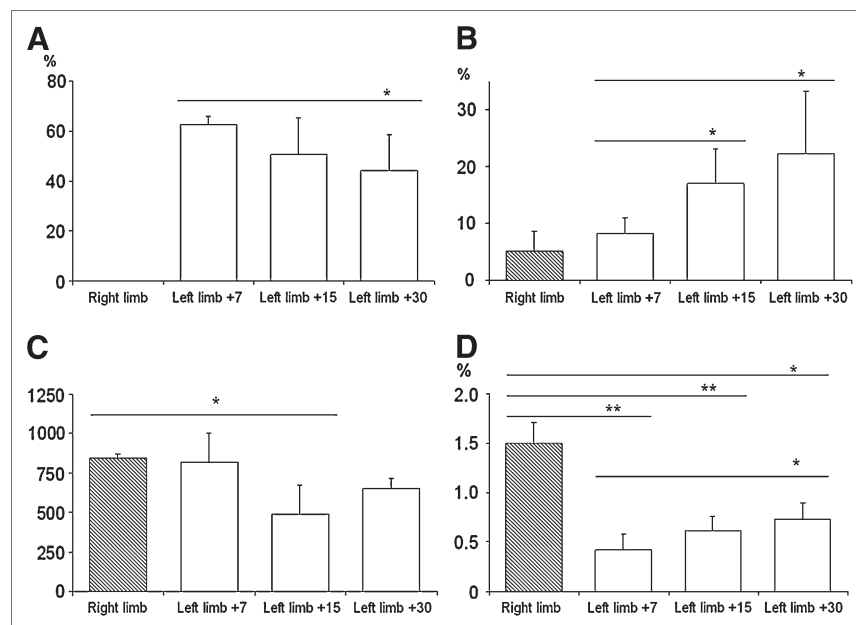
vascular sites, often containing atherosclerotic disease (*34*). Similarly, other comorbid illnesses frequently associated with human PAOD (diabetes, hypertension, hypercholesterolemia) are usually absent in animal models. Some studies have addressed some of these facts by performing the ligation in diabetic (*35*), hypercholesterolemic (*36–38*), hyperhomocysteinemic (*38*), and aged (*39*) mice. Our study really validates the use of ^{13}N-ammonia PET in acute and subacute models and not in chronic disease. Thus, on the basis of the current study, validation of ^{13}N-ammonia PET in animal models that better represent the human disease is warranted.

Our study also provides useful information with regard to the histologic analysis after acute hindlimb ischemia in a mouse model of PAOD. In most preclinical models, changes in perfusion at the histologic level have been performed by measuring capillary density. However, capillary density may be increased paradoxically in patients with PAOD—as a potentially beneficial adaptation and as an attempt to compensate for the reductions in blood flow (*10*)—so that other histologic assessments may be needed to examine the benefit of the therapeutic strategy being used. In accordance with the functional recovery observed in the ischemic limb, there was a partial reduction in the amount of necrosis 1 mo after the ischemic insult, which was also associated with an improvement in the area occupied by arterioles, but there was no reduction in the amount of fibrosis. Interestingly, the significant correlation between necrosis, fibrosis, and ^{13}N-ammonia uptake suggests that small-animal PET may actually provide information not only about perfusion but also about the functionality of the ischemic muscle. These results should be a valuable tool to determine the potential effect of specific therapies designed to treat PAOD of the limb.

However, this model of femoral or iliac artery ligation in nude mice is not entirely representative of what happens in critical limb ischemia in humans, where the process is more chronic because of the progressive arterial obstruction caused by growth of atherosclerotic lesions, and our results might not be extrapolated readily to human pathology. Furthermore, the healing process in an unaffected limb—more so in mice—is associated with a different degree of spontaneous recovery as we have shown herein (Fig. 4), which again is not the case in human disease. To avoid these issues the use of more severely damaged animals, such as apolipoprotein E or certain transgenic animal models, could better represent human disease. Part of our current investigation is to analyze the therapeutic benefit of cell therapy.

Notwithstanding these issues, as the goal of the study was to validate the use of small-animal PET for assessment of limb ischemia—even acute—and as we demonstrate a good correlation between histologic and the small-animal PET technique, we believe that it is reasonable to conclude that small-animal PET can be useful in this setting.

CONCLUSION

We demonstrate that ^{13}N-ammonia imaging allows for evaluation of hindlimb perfusion in surgical mouse models of hindlimb ischemia, providing a useful tool for assessment of new therapeutic strategies for hindlimb ischemic disease. Although both I and F models are associated with spontaneous recovery, perfusion recovery in the I model is only partial and, thus, should provide a better model for therapeutic assessment of novel strategies for treatment of PAOD.

ACKNOWLEDGMENTS

REFERENCES

1. Criqui MH, Fronek A, Barrett-Connor E, Klauber MR, Gabriel S, Goodman D. The prevalence of peripheral arterial disease in a defined population. *Circulation.* 1985;71:510–515.

2. Ouriel K. Peripheral arterial disease. *Lancet.* 2001;358:1257–1264.

3. Baumgartner I, Schainfeld R, Graziani L. Management of peripheral vascular disease. *Annu Rev Med.* 2005;56:249–272.

4. Regensteiner JG, Hiatt WR. Current medical therapies for patients with peripheral arterial disease: a critical review. *Am J Med.* 2002;112:49–57.

5. A prospective epidemiological survey of the natural history of chronic critical leg ischaemia. The I.C.A.I. Group (gruppo di studio dell'ischemia cronica critica degli arti inferiori). *Eur J Vasc Endovasc Surg.* 1996;11:112–120.

6. Tateishi-Yuyama E, Matsubara H, Murohara T, et al. Therapeutic angiogenesis for patients with limb ischaemia by autologous transplantation of bone-marrow cells: a pilot study and a randomised controlled trial. *Lancet.* 2002;360:427–435.

7. Yoon CH, Hur J, Park KW, et al. Synergistic neovascularization by mixed transplantation of early endothelial progenitor cells and late outgrowth endothelial cells: the role of angiogenic cytokines and matrix metalloproteinases. *Circulation.* 2005;112:1618–1627.

8. Lekas M, Lekas P, Latter DA, Kutryk MB, Stewart DJ. Growth factor-induced therapeutic neovascularization for ischaemic vascular disease: time for a re-evaluation? *Curr Opin Cardiol.* 2006;21:376–384.

9. Waters RE, Terjung RL, Peters KG, Annex BH. Preclinical models of human peripheral arterial occlusive disease: implications for investigation of therapeutic agents. *J Appl Physiol.* 2004;97:773–780.

10. Hiatt WR, Hoag S, Hamman RF. Effect of diagnostic criteria on the prevalence of peripheral arterial disease: The San Luis Valley Diabetes Study. *Circulation.* 1995;91:1472–1479.

11. Buschmann IR, Voskuil M, van Royen N, et al. Invasive and non-invasive evaluation of spontaneous arteriogenesis in a novel porcine model for peripheral arterial obstructive disease. *Atherosclerosis.* 2003;167:33–43.

12. McDermott MM, Greenland P, Liu K, et al. The ankle brachial index is associated with leg function and physical activity: the Walking and Leg Circulation Study. *Ann Intern Med.* 2002;136:873–883.

13. Ubbink DT, Tulevski II, den Hartog D, Koelemay MJ, Legemate DA, Jacobs MJ. The value of non-invasive techniques for the assessment of critical limb ischaemia. *Eur J Vasc Endovasc Surg.* 1997;13:296–300.

14. Bajnok L, Kozlovszky B, Varga J, Antalffy J, Olvaszto S, Fulop T Jr. Technetium-99m sestamibi scintigraphy for the assessment of lower extremity ischaemia in peripheral arterial disease. *Eur J Nucl Med.* 1994;21:1326–1332.

15. Duet M, Virally M, Bailliart O, et al. Whole-body ^{201}Tl scintigraphy can detect exercise lower limb perfusion abnormalities in asymptomatic diabetic patients with normal Doppler pressure indices. *Nucl Med Commun.* 2001;22:949–954.

16. Hamanaka D, Odori T, Maeda H, Ishii Y, Hayakawa K, Torizuka K. A quantitative assessment of scintigraphy of the legs using ^{201}Tl. *Eur J Nucl Med.* 1984;9:12–16.

17. Miles KA, Barber RW, Wraight EP, Cooper M, Appleton DS. Leg muscle scintigraphy with 99Tcm-MIBI in the assessment of peripheral vascular (arterial) disease. *Nucl Med Commun.* 1992;13:593–603.

18. Murohara T, Asahara T, Silver M, et al. Nitric oxide synthase modulates angiogenesis in response to tissue ischemia. *J Clin Invest.* 1998;101:2567–2578.

19. Baumgartner I, Thoeny HC, Kummer O, et al. Leg ischemia: assessment with MR angiography and spectroscopy. *Radiology.* 2005;234:833–841.

20. Kusmierek J, Dabrowski J, Bienkiewicz M, Szuminski R, Plachcinska A. Radionuclide assessment of lower limb perfusion using ^{99m}Tc-MIBI in early stages of atherosclerosis. *Nucl Med Rev Cent East Eur.* 2006;9:18–23.

21. Surti S, Karp JS, Perkins AE, et al. Imaging performance of A-PET: a small animal PET camera. *IEEE Trans Med Imaging.* 2005;24:844–852.

22. Celen YZ, Zincirkeser S, Akdemir I, Yilmaz M. Investigation of perfusion reserve using 99Tc(m)-MIBI in the lower limbs of diabetic patients. *Nucl Med Commun.* 2000;21:817–822.

23. Luttun A, Lupu F, Storkebaum E, et al. Lack of plasminogen activator inhibitor-1 promotes growth and abnormal matrix remodeling of advanced atherosclerotic plaques in apolipoprotein E-deficient mice. *Arterioscler Thromb Vasc Biol.* 2002;22:499–505.

24. Couffinhal T, Silver M, Zheng LP, Kearney M, Witzenbichler B, Isner JM. Mouse model of angiogenesis. *Am J Pathol.* 1998;152:1667–1679.

25. Heil M, Schaper W. Influence of mechanical, cellular, and molecular factors on collateral artery growth (arteriogenesis). *Circ Res.* 2004;95:449–458.

26. Bellina CR, Parodi O, Camici P, et al. Simultaneous in vitro and in vivo validation of nitrogen-13-ammonia for the assessment of regional myocardial blood flow. *J Nucl Med.* 1990;31:1335–1343.

27. Schelstraete K, Simons M, Deman J, Vermeulen FL, Goethals P, Bratzlavsky M. Visualization of muscles involved in unilateral tremor using ^{13}N-ammonia and positron emission tomography. *Eur J Nucl Med.* 1982;7:422–425.

28. Tack CJ, van Gurp PJ, Holmes C, Goldstein DS. Local sympathetic denervation in painful diabetic neuropathy. *Diabetes.* 2002;51:3545–3553.

29. Seder JS, Botvinick EH, Rahimtoola SH, Goldstone J, Price DC. Detecting and localizing peripheral arterial disease: assessment of ^{201}Tl scintigraphy. *AJR.* 1981;137:373–380.

30. Dabrowski J, Mikosinski J, Kusmierek J. Scintigraphic and ultrasonographic assessment of the effect of lumbar sympathectomy upon chronic arteriosclerotic ischaemia of lower extremities. *Nucl Med Rev Cent East Eur.* 2003;6:17–22.

31. Sayman HB, Urgancioglu I. Muscle perfusion with technetium-MIBI in lower extremity peripheral arterial diseases. *J Nucl Med.* 1991;32:1700–1703.

32. Li W, Shen W, Gill R, et al. High-resolution quantitative computed tomography demonstrating selective enhancement of medium-size collaterals by placental growth factor-1 in the mouse ischemic hindlimb. *Circulation.* 2006;113:2445–2453.

33. Pu LQ, Jackson S, Lachapelle KJ, et al. A persistent hindlimb ischemia model in the rabbit. *J Invest Surg.* 1994;7:49–60.

34. Boger RH, Bode-Boger SM, Thiele W, Creutzig A, Alexander K, Frolich JC. Restoring vascular nitric oxide formation by L-arginine improves the symptoms of intermittent claudication in patients with peripheral arterial occlusive disease. *J Am Coll Cardiol.* 1998;32:1336–1344.

35. Rivard A, Silver M, Chen D, et al. Rescue of diabetes-related impairment of angiogenesis by intramuscular gene therapy with adeno-VEGF. *Am J Pathol.* 1999;154:355–363.

36. Couffinhal T, Silver M, Kearney M, et al. Impaired collateral vessel development associated with reduced expression of vascular endothelial growth factor in ApoE-/- mice. *Circulation.* 1999;99:3188–3198.

37. Duan J, Murohara T, Ikeda H, et al. Hypercholesterolemia inhibits angiogenesis in response to hindlimb ischemia: nitric oxide-dependent mechanism. *Circulation.* 2000;102:III370–III376.

38. Duan J, Murohara T, Ikeda H, et al. Hyperhomocysteinemia impairs angiogenesis in response to hindlimb ischemia. *Arterioscler Thromb Vasc Biol.* 2000;20:2579–2585.

39. Rivard A, Fabre JE, Silver M, et al. Age-dependent impairment of angiogenesis. *Circulation.* 1999;99:111–120.